Experimental study of high-temperature smectic-C^*_{FI2} phase in chiral smectic liquid crystals that exhibit phase-sequence reversal

K. L. Sandhya,[1] J. K. Song,[1] Yu. P. Panarin,[1,2] J. K. Vij,[1,*] and S. Kumar[3]
[1]*Department of Electronic and Electrical Engineering, Trinity College, University of Dublin, Dublin 2, Ireland*
[2]*School of Electrical and Communication Engineering, Dublin Institute of Technology, Dublin 8, Ireland*
[3]*Raman Research Institute, Bangalore, 560 080, India*
(Received 26 October 2007; published 29 May 2008)

We report the results of an experimental study of a recently observed phase sequence reversal of smectic-C^*_{FI2} [SmC^*(q_T=1/2); a four layer antiferroelectric] phase appearing in the temperature range above the smectic-C^* (SmC^*) phase from the results of optical birefringence, spontaneous polarization, selective reflection, conoscopy, and dielectric spectroscopy. The SmC^*_{FI2} phase is observed in an antiferroelectric liquid crystalline compound, 10OHF, in a temperature range above that of SmC^* phase and is found to be thermodynamically monotropic, i.e., it appears only upon cooling from SmC^*_α phase. This is also unstable as if it is once transformed to SmC^* by the application of the bias, it does not return to its original state unless the sample is heated and cooled again in the absence of the bias. Nevertheless this phase is stabilized by the addition of a chiral smectic compound 9OTBBB1M7 (abbreviated as C9), having a wide temperature range of the SmC^*_{FI2} phase. The temperature range of the low temperature SmC^* decreases with increase in the concentration of C9 and for a concentration of 55 wt. %, SmC^* disappears and the transition takes place directly from SmC^*_{FI2} to the crystalline phase on cooling. The existence of such a high-temperature SmC^*_{FI2} phase is also supported by a phenomenological model.

DOI: 10.1103/PhysRevE.77.051707 PACS number(s): 61.30.Gd, 77.84.Nh

I. INTRODUCTION

Discovery of aniferroelectricity [1] in liquid crystals has led to intensive research into detailed studies of the anticlinic SmC^*_A phase, which has resulted in the identification of the various ferrielectric subphases (FI1 and FI2) including that of the SmC^*_α phase in a temperature range between the antiferroelectric (SmC^*_A) and Sm*A* phases [2]. The appearance of these subphases can be understood to be result of a competition between the antiferroelectric (AF) and ferroelectric (F) interactions in the adjacent smectic layers. According to Osipov and Fukuda model, subphases observed in the chiral systems arise from the long-range interactions of the polarizations of the layers. The polarization of a layer is a combination of the polarizations from chirality and the discrete flexoelectricity [3,4]. Discrete flexoelectric polarization arises from an azimuthal arrangement of molecules in the next to the nearest neighboring layers. A direct study using resonant x-ray diffraction [4,5] has found a nonplanar short-pitch distorted clock (or distorted Ising) structure of these subphases, where the azimuthal angle (φ) changes at a constant value from the layer to layer. These subphases are characterized by the short-pitch periodicity of an integral number of layers in a unit cell for subphases other than SmC^*_α. The SmC^*_α phase has a temperature-dependent periodicity ranging from 3 to 8 layers [4–6]. A typical phase sequence observed in antiferroelectric liquid crystals is Sm*A*-SmC^*_α-SmC^*-SmC^*_{FI2} (four-layer periodicity or q_T=1/2)-SmC^*_{FI1} (three-layer or q_T=1/3)-SmC^*_A (two-layer or q_T=0) on decreasing the temperature. q_T is defined as the fraction of synclinic order to the total synclinic and anticlinic orders in a unit cell. Designations of these subphases as SmC^*_A(q_T) with q_T varying from 0 to 1 is useful since subphases other than 3 and 4 layers can be accommodated within this scheme. q_T=0 and 1 correspond to SmC^*_A and SmC^*, respectively. In some systems some of the subphases may be missing, but if they exist they will always appear in the same phase sequential order upon cooling. In addition to this well-established order, other ferrielectric subphases with longer short pitch layer periodicity have also been observed [7].

Recently Wang *et al.* [8] reported the existence of a phase sequence reversal in a compound 10OHF using the technique of null transmission ellipsometry and its binary mixtures with 9OTBBB1M7 (abbreviated as C9) by employing both null transmission ellipsometry and resonant x-ray diffraction techniques. They observed SmC^*_{FI2} phase above the temperature range of SmC^* phase. They tentatively explained the observed phase sequence reversal behavior by the two recently developed phenomenological models [9,10]. In our comment [11] to their paper [8], we reported that in the pure 10OHF compound the high-temperature SmC^*_{FI2} phase is metastable and both SmC^* and SmC^*_{FI2} phases are monotropic, i.e., they exist only upon cooling. Here we report a study on the pure 10OHF sample and the binary mixtures of 10OHF with 9OTBBB1M7 (called C9) using a range of complementary techniques and confirm the phase sequence reversal SmC^*_α-SmC^*_{FI2}-SmC^* occurs under certain conditions. Results of our experimental study on the pure 10OHF and its binary mixtures show that both SmC^* and SmC^*_{FI2} are monotropic in the pure sample while these become thermodynamically stable in the binary mixtures with the compound C9.

*jvij@tcd.ie

(a) 10OHF

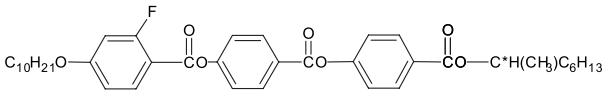

Iso 120.7 °C Sm*A* 82.5 °C SmC_α* 72.9 °C SmC_{FI2}*(?) 61.4 °C SmC* 55.5 °C Cr

(b) 9OTBBB1M7 (C9)

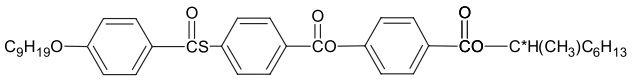

Iso 150.8 °C Sm*A* 111.9 °C SmC_α* 103.6 °C SmC_{FI2}* 86.9 °C SmC_A* 68.9 °C Cr

FIG. 1. Chemical structures of the compounds used in the investigations, (a) 10OHF and (b) 9OTBBB1M7 (C9).

II. EXPERIMENT

The chemical structure of the compounds 10OHF and C9 are shown in Fig. 1. We use a range of techniques: electric field induced optical birefringence, dielectric spectroscopy, polarization, conoscopy, and the selective reflection to investigate the existence of the phase sequence reversal in 10OHF and binary mixtures of 10OHF with C9. The dielectric and polarization measurements are carried out on a liquid crystalline sample sandwiched in between two indium tin oxide (ITO) coated glass plates. These plates were treated with a polyimide solution and rubbed unidirectionally for planar alignment. The cell gap using Mylar spacers was fixed at 26 μm. For conoscopy measurements, a homeotropically aligned cell of thickness 75 μm has been used. Aluminum foil strips separated by 300 μm are used as electrodes. The aligning agents (i) polyimide RN1175 (Nissan Chemical Ind., Ltd.) and (ii) carboxylato chromium complexes (chromolane) are used to obtain the planar and homeotropic alignments, respectively. The cells are filled in the isotropic phase by the capillary action. The temperature of the cell kept in the hot stage is varied using Eurotherm temperature controller 2604 with an accuracy of 0.01 °C.

Dielectric measurements are carried out in the frequency range 10 Hz–10 MHz using a Novocontrol broadband dielectric spectrometer. Spontaneous polarization is measured using the integral reversed current method [12]. The conoscopic image quality deteriorated seriously when some liquid crystal flow was observed to occur. To avoid or minimize any flow of the liquid crystalline sample occurring, a rectangular shaped voltage of frequency 1 Hz is used instead of the dc voltage. A function generator along with the amplifier allowed us to apply voltage up to 200 V corresponding to a field of 2 V/μm. The selective Bragg reflection band for a homeotropic cell of thickness 31 μm was measured at an oblique angle of incidence of 20° using an UV–visible–near-IR spectrophotometer (Perkin Elmer, Lambda 900).

The electric-field induced birefringence measurement is carried out on the sample aligned in homeotropic geometry.

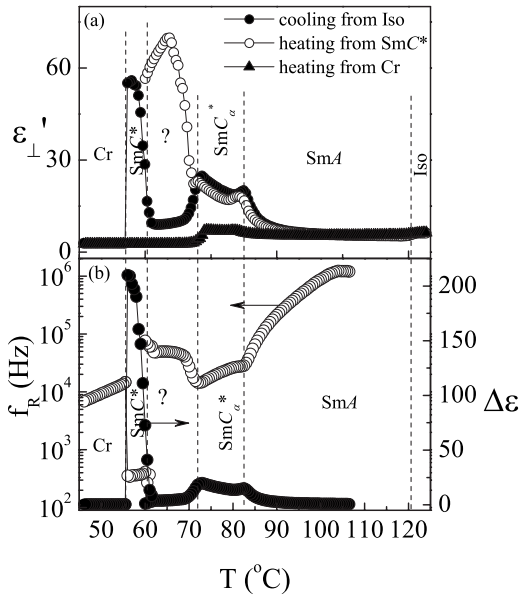

FIG. 2. (a) Temperature dependence of the real part of dielectric permittivity $\epsilon_\perp'$ at 1 kHz in the cooling and heating modes and (b) temperature dependence of the relaxation parameters f_R (Hz) (○) and $\Delta\epsilon$ (●) for 10OHF.

This involves the use of a photoelastic modulator (PEM) [7]. This measurement is carried out to rule out the possibility of the surface effect playing any role in giving rise to the phase sequence reversal. The homeotropic cell of thickness 25 μm is used for the purpose. The bottom plate is designed to have two ITO strips spaced by 180 μm from each other and these are used to apply the in-plane electric field parallel to the smectic layers. The top cover glass plate in this case is without the ITO layer. The temperature of the cell is varied with a step of 0.1 °C allowing a 1 min. waiting time for stabilization of each temperature before recording the measurements. For the dielectric measurements Novocontrol temperature control system is used to vary the temperature of the sample. We find a slight temperature difference between the dielectric measurements and the other experiments reported in this paper as these use different hot stages at relatively higher temperatures.

III. RESULTS AND DISCUSSIONS

A. Investigation on pure 10OHF sample

1. Dielectric spectroscopy measurements

Figure 2(a) shows the temperature dependence of the dielectric permittivity $\epsilon_\perp'$ on cooling and heating for a fixed frequency of 1 kHz and Fig. 2(b) presents the temperature dependence of the relaxation parameters. To extract the parameters characterizing the relaxation process, the data were fitted to the Havriliak-Negami expression

$$\epsilon^*(\omega) = \epsilon_\infty + \sum_{j=1}^{n} \frac{\Delta\epsilon_j}{[1 + (i\omega\tau_j)^\alpha]^\beta}. \quad (1)$$

Here $\epsilon^*(\omega)$ is the frequency dependent complex permittivity, $\omega = 2\pi f$; f is the measuring frequency, ϵ_∞ is the high-

frequency permittivity, j is a variable denoting the number of the relaxation processes up to n. τ_j is the relaxation time and $\Delta\epsilon_j$ is the dielectric relaxation strength for the jth process. The parameters α and β describe the width and the asymmetric broadening of the dielectric loss curve; $\alpha=\beta=1$ leads to the Debye relaxation process. We find that over an entire temperature range of the dielectric measurements $\beta=1$. This indicates that the loss curves are symmetric about the maximum value of the dielectric loss. The parameter α has been found to lie in between 0.8 and 0.99 signifying the distribution of the relaxation times to be quite narrow. In a temperature range of 82 to 72 °C, dielectric permittivity ($\epsilon'_\perp$) shows a typical signature of SmC^*_α. Dielectric permittivity increases on approaching the SmA-SmC^*_α phase transition both from the low and high temperature sides. Such a feature is attributed to the soft mode caused by the tilt angle fluctuations and it exhibits a similar behavior for the SmC^*_α-SmC^*_{FI2} transition. In other words, $\Delta\epsilon$ decreases and f_R increases away from the transition temperature [Fig. 2(b)]. Dielectric permittivity drops rapidly at a temperature of 72 °C and it has a very low value within the temperature range of 70 to 61 °C. This weak dielectric response points to a low or even almost zero value of the macroscopic spontaneous polarization. This is caused by the polarization of the individual layers canceling out with each other in a unit cell to give rise to an antiferroelectric structure for the SmC^*_{FI2} phase. The temperature-independent high-frequency mode of weak strength observed here [Fig. 2(b)] is also a typical signature of the SmC^*_{FI2} phase. This mode can be understood to be an azimuthal antiphase reorientation of the molecular directors with a constant tilt angle [13]. At a temperature of 61 °C the dielectric permittivity starts to increase giving rise to a large value in the temperature range 61 to 55 °C. The relaxation process observed in this temperature range is attributed to the existence of ferroelectric Goldstone mode [14]. Some rather weak relaxation is also observed in the crystalline phase due to a flip-flop tumbling of the molecules around the short axis. Dielectric measurements carried out for the cooling cycle confirm that SmC^*_{FI2} phase exists over a higher temperature range than SmC^* phase.

The temperature dependence of dielectric permittivity for a fixed frequency of 1 kHz in the heating cycle with and without going to crystallization is also shown in Fig. 2(a). When the sample is heated from a temperature higher than the crystalline phase, i.e., from the low-temperature SmC^* phase, the data show the disappearance of a four-layer phase in the temperature range 70 to 61 °C. The large permittivity indicates that the phase under investigation is SmC^*, i.e., SmC^*_{FI2} phase is monotropic. On heating from the crystallization temperature both SmC^*_{FI2} and SmC^* disappear and the sample directly goes into SmC^*_α phase. Hence SmC^* phase is also monotropic, i.e., it exists only during the cooling mode and consequently the phase sequence reversal SmC^*_α-SmC^*_{FI2}-SmC^* is exhibited in the cooling cycle only.

2. Effect of the bias voltage on SmC^*_{FI2} phase

To check the stability of this high-temperature SmC^*_{FI2} phase we measure $\epsilon'_\perp$ with the field applied. Figure 3 shows the dependence of $\epsilon'_\perp$ on bias field for a frequency of 1 kHz

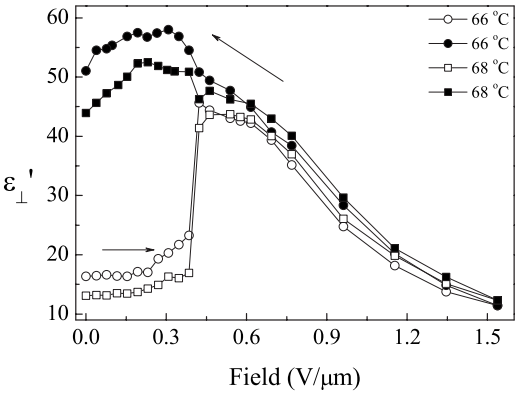

FIG. 3. Dielectric permittivity $\epsilon'_\perp$ at a frequency of 1 kHz for SmC^*_{FI2} phase as a function of the bias field for 10OHF. Open and closed symbols represent the increasing and decreasing bias fields, respectively. Note that on decreasing the bias field $\epsilon'_\perp$ value does not come back to its original value.

in SmC^*_{FI2} phase. The sample is cooled to SmC^*_{FI2} from SmA phase without any voltage applied across the cell and then voltage is increased from 0 to 40 V and decreased back to 0 V. The results show that at a field of ~0.38 V/μm the dielectric permittivity increases since the compound in SmC^*_{FI2} phase transforms to the unwound SmC^* phase and it does not return to its initial state while the bias is reversed. It stays in the SmC^* phase unless it is heated to SmC^*_α and cooled back to SmC^*_{FI2} phase without any field applied across the cell. Hence the high-temperature SmC^*_{FI2} phase is also metastable. This conclusion is supported by the measurements on spontaneous polarization and conoscopy and will be presented later.

3. Polarization measurements

Figure 4(a) shows the normalized spontaneous polarization as a function of the field in the various phases of the material. At a temperature of 76 °C, corresponding to the SmC^*_α phase the polarization normalized to its maximum value shows a typical signature of SmC^*_α phase. Up to a field 0.25 V/μm the spontaneous polarization is very small and increases linearly with voltage and at the critical field of 0.27 V/μm, the field starts unwinding the helix and hence the polarization increases and finally saturates to a constant value. The spontaneous polarization plot corresponding to SmC^*_{FI2} phase (66 and 64 °C) shows a typical signature of SmC^*_{FI2} phase [13] where the macroscopic spontaneous polarization shows a very low threshold electric field. Below the critical field the polarization is zero and at the critical field the short helix of SmC^*_{FI2} transforms to helical SmC^* and then long helix is distorted and starts unwinding with the result that the macroscopic polarization starts increasing and finally reaches a saturation value of Ps. At a temperature 57 °C, the behavior is reminiscent of SmC^* phase, having no threshold. Thus in the two temperature ranges mentioned above, the dielectric and polarization data reflect typical signatures for both the SmC^*_{FI2} and SmC^* phases. Figure 4(b) shows spontaneous polarization normalized to its saturation value at 66 °C (initially in the SmC^*_{FI2} phase) with increas-

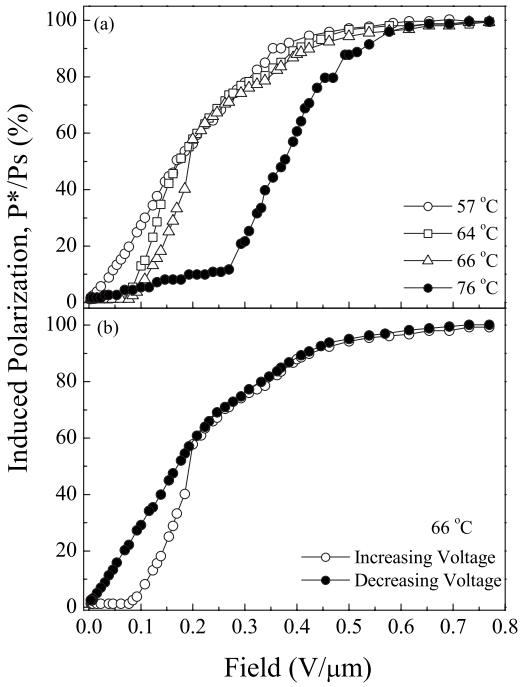

FIG. 4. (a) Temperature dependence of the spontaneous normalized polarization as a function of field increasing for different phases for 10OHF: SmC^*_α (76 °C); SmC^*_{FI2} (66 and 64 °C) and SmC^* (57 °C). (b) The normalized spontaneous polarization as a function of the bias field at 66 °C (initially at SmC^*_{FI2}) measured during the increase (○), and decrease (●) in the bias field back to zero bias field.

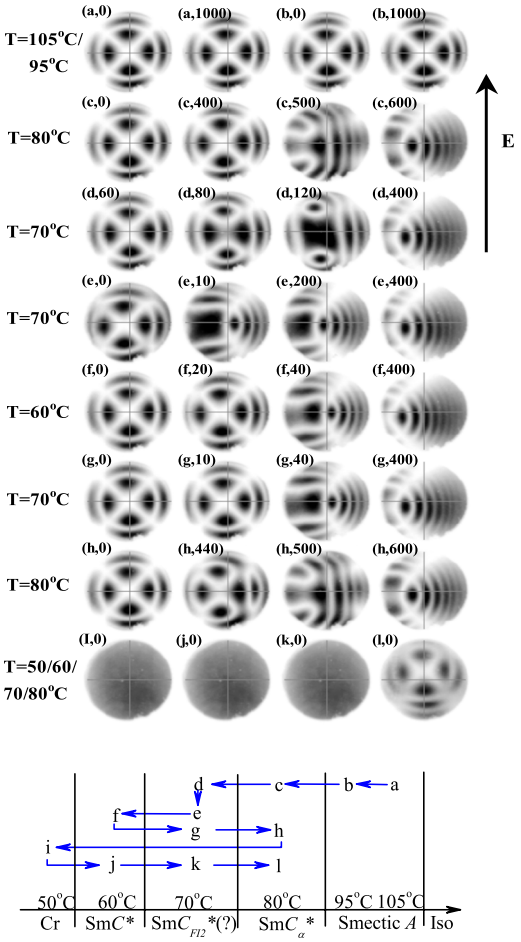

FIG. 5. (Color online) Conoscopy as a function of temperature and the applied field (1 Hz, rectangular wave is applied) for 10OHF. Experiments were carried out on the following temperature sequence: (a) 105 °C (SmA)→(b), 95 °C (SmA)→(c), 80 °C (SmC^*_α)→(d), 70 °C (SmC^*_{FI2})→(e), 70 °C (SmC^*)→(f), 60 °C (SmC^*)→(g), 70 °C (SmC^*)→(h), 80 °C (SmC^*_α)→(i), 50 °C (Cr)→(j), 60 °C (Cr)→(k), 70 °C (Cr)→(l), 80 °C (SmC^*_α). The numbers in images of (a)–(l) show the amplitude of the applied field (V/mm). The lower part of the figure shows the sequence of temperature in which experiments were carried out.

ing and decreasing field. With increasing field it shows the characteristics of SmC^*_{FI2} phase have a low threshold and an application of field greater than the threshold transforms it to ferroelectric SmC^* phase. On reversing the field, it shows characteristics of SmC^* having no threshold. This confirms the result obtained from dielectric measurements that once the sample transforms to the SmC^* phase it stays there even though the field was removed. Consequently SmC^*_{FI2} is not stable.

4. Conoscopy measurements

To rule out the possibility of the surface effects playing a role in giving rise to the phase reversal behavior in a planar cell, conoscopy was studied using a homeotropic cell with the sample thickness of 75 μm. The sample is first cooled slowly from 105 to 70 °C on a scheme shown in Fig. 5 and conoscopic images are recorded for temperatures of 105, 95, 80, 70, again at 70 °C after the large field had been applied and removed and then cooled to 60 °C. The sample is then heated and conoscopic images recorded at 70, 80 °C, then cooled to 50 °C in the crystalline phase and then heated back again to 80 °C while recording images at temperatures of 60, 70, and 80 °C. For each of these temperatures, the field is increased as specified in Fig. 5 in V/mm in the parenthesis. Figures 5(a) and 5(b) show a typical conoscopic image for SmA phase. Figures 5(c) and 5(h) at a temperature of 80 °C show typical images of SmC^*_α where the unwinding of helix requires relatively high fields and the intermediate state exhibits large negative biaxiality increasing with an increase in the tilt angle [15]. Figures 5(e) at temperature of 70 °C, Fig. 5(f) at a temperature of 60 °C during the first cooling cycle, and Fig. 5(g) at a temperature of 70 °C during the heating cycle show a typical signature of SmC^* phase [4,16]. The unwinding of SmC^* phase has no threshold and the center of the image shifts in a direction normal to the applied field and its shift increases with an increase in the field. The structure becomes increasing biaxial with an increase in the apparent tilt angle, and the optical plane containing the optical axes continues to be perpendicular to the direction of the applied field. Figure 5(d) taken for a temperature of 70 °C for different voltages exhibit a slight threshold (note that the conoscopic image at a field of 60 V/mm is the same as for 0 V/mm) and exhibits biaxiality without tilting (note that the image at 80 V/mm has no tilt but has biaxiality and the image at 120 V/mm indeed shows

very large biaxiality but the tilt angle is still rather low). This is the typical signature of a SmC^*_{FI2} phase [4,17]. Once the structure is completely unwound it then transforms to ferroelectric SmC^* phase and it stays there in that state [image (e)] unless it is cooled from SmC^*_α again. If the sample is heated from the low temperature phase, SmC^* (60 °C), it still showed the behavior similar to SmC^* [image (g)] at a temperature 70 °C where SmC^*_{FI2} would have normally appeared under the cooling cycle. Note that image (e) shows initially rapid unwinding compared to that of the image (g). This is because image (e) was recorded just after removing the field, i.e., just after taking the image (d). Usually, after applying the field in a homeotropic cell of SmC^* phase and turning off the field, the sample does not return to a perfectly coiled initial helical structure, but it contains defects or disclination lines. The disclination lines imply that the helical fractures that have occurred during the helical unwinding process persist after the field has been removed. Especially, in this material, we think that the energy difference between the synclinic and anticlinic states is somewhat lower than in the usual ferroelectric materials, and more disclination lines can persist easily after turning off the field. Therefore, the state (e,0) at zero field is not a perfect helical structure, but a slightly distorted helix. We observed the slightly tilted image of (e,0) compared with other images at zero field. The slightly distorted helical structure can easily be unwounded by applying the field. This makes a slight difference in the images. On the other hand, (g) is obtained by heating the cell slowly from 60 °C with an almost perfect helical structure. When the sample is heated from the crystalline phase it goes directly in to SmC^*_α phase at a temperature 80 °C indicating the absence of both SmC^* and SmC^*_{FI2} phases [images (i)–(l)] in the heating mode. Even though the conoscopic figures at 70 °C [image 5(d)] show signature similar to those of a SmC^*_{FI2} phase, the signature is not that of a typical SmC^*_{FI2} phase reported in the literature [4]. With the application of field, the melatopes are not perpendicular to the field contrary to what is usually observed for such a phase. We rather observe behavior similar to a ferrielectric phase (SmC^*_{FI1}) where the melatopes are parallel to the field. Two reasons for this behavior are possible. The first reason is that the molecules in a synclinic arrangement within a layer flip due to thermal defects. Miyachi *et al.* [18] observed the disordered and the fluctuating feature in the laser diffraction of SmC^*_{FI1} phase. They explained it by considering the flipping of the molecules in the interlayer molecular arrangement at some places in the smectic layers. The same phenomenon may also occur in SmC^*_{FI2}. This will create an effective in-plane spontaneous polarization perpendicular to the tilt plane. Such a flipping of the molecules can easily occur thermally, because it does not alter the total number of the anticlinic (A) and synclinic (S) orderings in a unit cell. The consecutive molecular arrangement of a unit cell *ASASASAS*… may become *ASSAASAS*…. The energy difference between these two molecular arrangements is very small, however the latter has an effective spontaneous polarization. This means that flip of the c directors of only one of the layers has given rise to this changed structure. The unit cell on the average has periodicity of four layers because such a defect may occur only in one out of say 100 layers.

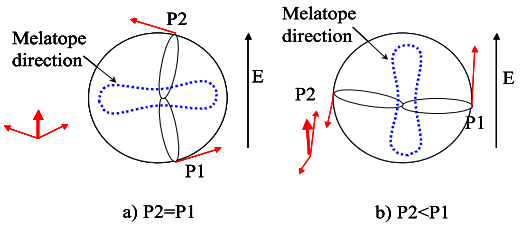

FIG. 6. (Color online) Schematic diagram illustrating the dependence of directions of melatopes on the residual polarization for (a) $P2=P1$ and (b) $P2<P1$.

This flipping of molecules in some parts of the smectic layers may be caused by the solitonlike wave motion. This will cause both the static and dynamic distortions in the helicoidal structure. It may not be possible to observe such a defect even using resonant x rays. The second reason may be that the SmC^*_{FI2} phase exhibited at high temperatures is unusual and is metastable, i.e., the stability of the high-temperature SmC^*_{FI2} phase is rather weak compared with the normal low-temperature SmC^*_{FI2} phase. The conscopic image obtained at 70 °C has a small tilt angle but a large biaxiality. Moreover, a slight threshold appears. The low threshold is a characteristic of SmC^*_{FI2} but not of the SmC^*_{FI1} phase. Therefore we conclude that phase under consideration is SmC^*_{FI2}. However, the observed direction of the melatopes is parallel to the applied field. The direction of the melatopes is determined by the residual polarization. In the SmC^*_{FI2} phase, the spontaneous polarization of each layer is almost canceled out by the opposite direction of the neighboring polarization, and a small residual polarization is almost parallel to the c director as shown in a schematic Fig. 6(a) However, when the symmetric balance is broken, that is, when one of the polarization vectors is larger than the other, the melatopes rotate as shown in Fig. 6(b). This may give rise to a disturbed structure for SmC^*_{FI2} phase as is observed here.

On comparing the results obtained from dielectric, polarization, conoscopy, selective reflection, and the polarizing microscopy, we arrive at the conclusion that the high temperature phase is a four-layer phase and exhibits the phase sequence reversal SmC^*_α-SmC^*_{FI2}-SmC^* in the cooling cycle. Summarizing we find that both the high temperature SmC^*_{FI2} phase and low-temperature SmC^* phase are monotropic and the high-temperature SmC^*_{FI2} is metastable. Once SmC^*_{FI2} is transformed in to SmC^* phase on the application of the electric field across the smectic layer or the system is heated from the SmC^* phase, the latter stays there and does not go back to its original state of SmC^*_{FI2} on the removal of the field. It can occur again only if the cell is cooled from SmC^*_α phase. Furthermore the conoscopic images of SmC^*_{FI2} are rather disturbed and exhibit some characteristics of SmC^*_{FI1}. To improve the stability of SmC^*_{FI2} phase we study the binary mixtures of 10OHF with C9.

B. Study of the binary mixtures

Figure 7(a) shows the temperature dependent relative permittivity at a frequency of 1 kHz carried out in the cooling mode for different concentrations of C9 with 10OHF (speci-

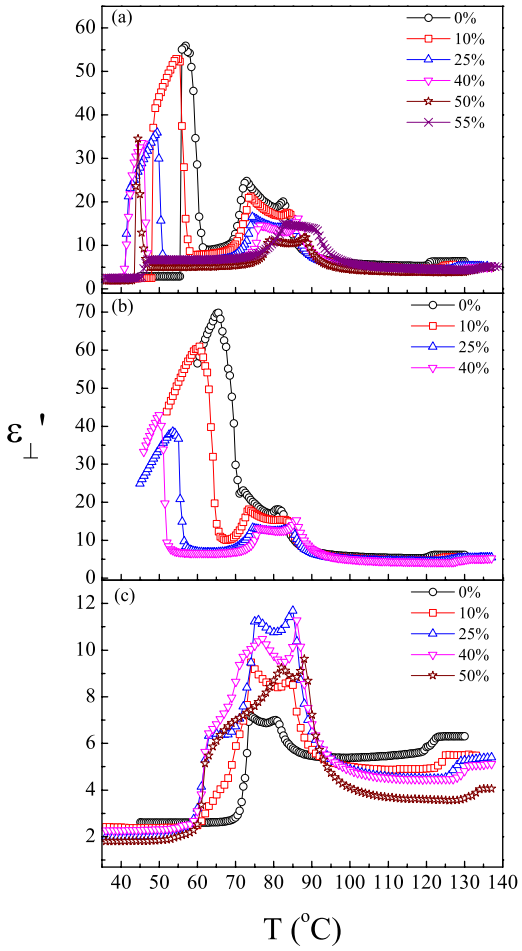

FIG. 7. (Color online) Temperature dependence of the dielectric permittivity $\epsilon_\perp'$ at a frequency of 1 kHz for different mixtures of C9 in 10OHF in the (a) cooling (b) heating modes. In the latter the sample is heated from the low temperature SmC^* phase and (c) sample heated from the crystalline phase.

fied by the value of the parameter X; for example $X=10$ denotes 10% by weight of C9 in 10OHF). It has been observed that the range of SmC^*_{FI2} phase increases with an increase in the concentration of C9. The range of the low-temperature SmC^* phase also increases initially, up to $X=25$ mixture, then it starts to decrease and finally for $X=55$ mixture SmC^* phase disappears. Hence there is no phase sequence reversal for $X=55$.

When the sample is heated from its SmC^* phase, the high-temperature SmC^*_{FI2} phase does not exist in the heating mode for $X=0$, as discussed earlier. However, it exists for $X=10$ and the temperature range increases with an increase in the concentration of C9 [see Fig. 7(b)]. We find that the temperature range of SmC^*_{FI2} phase in the heating mode is less wide compared to that during the cooling cycle. When the sample is heated from the crystalline the low temperature SmC^* does not exist even in the mixture [Fig. 7(c)] and hence the SmC^* phase is monotropic.

To check the stability of high temperature SmC^*_{FI2} phase and to avoid the surface effects playing a role in a planar cell, the electric field induced birefringence measurement was carried out using a photoelastic modulator for a sample

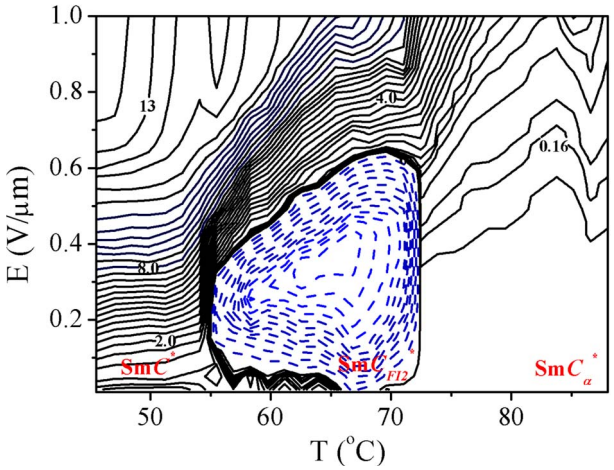

FIG. 8. (Color online) The electric-field-induced birefringence observed in the cooling mode for 40 wt. % of C9 in 10OHF. Birefringence contours shown as the dotted blue lines denote unwinding of the macroscopic helices of SmC^*_{FI2} phase. The birefringence contours drawn are in step of $\Delta n=0.5\times10^{-3}$

in a homeotropic cell of thickness 25 μm. Figure 8 shows the E-T phase diagram of the electric-field-induced birefringence for $X=40$ obtained in the cooling mode. Clearly, each phase shows its characteristic pattern of the birefringence contours [7]. SmC^*_α phase experiences field-induced deformations much greater than those experienced by SmA phase when the field is applied and hence can be identified easily. The birefringence contours show some dents or valleys just below SmA phase and the extrapolation to the zero field indicates SmA-SmC^*_α transition. Because of the short pitch helical structure the unwinding process in SmC^*_α phase requires high threshold field and becomes lower as the temperature decreases due to the pitch becoming longer. In SmC^*_{FI2} phase the in-layer directors first tend to become parallel to the applied field during the unwinding process. Accordingly, the birefringence goes negative and forms negative peaks in the birefringence contours as shown by the blue dotted lines in Fig. 8. The SmC^*_{FI2} phase requires a relatively small field for the unwinding of the helix and hence can easily be distinguished from SmC^*_A phase and this rules out the possibility of the phase being a two-layer instead of a four-layer SmC^*_{FI2} phase. At higher fields the birefringence contours are oblique and as the temperature decreases, the slope of the line decreases indicating birefringence increases with the field. In the SmC^* phase at lower field the contours are almost parallel to the temperature axis and at higher fields the contours get parallel to the electric field axis indicating that the birefringence is almost saturated with the field.

Figure 9 shows the phase diagram obtained for the binary mixture in the cooling mode. The points are determined from the temperature dependence of the dielectric permittivity $\epsilon_\perp'$ on cooling for a fixed frequency of 1 kHz, i.e., these have been deduced from Fig. 7(a). The range of high temperature phase SmC^*_{FI2} increases with an increase in concentration of C9. For $X=55$, the low-temperature SmC^* phase disappears and exhibits the transition from SmC^*_{FI2} to crystalline. Note

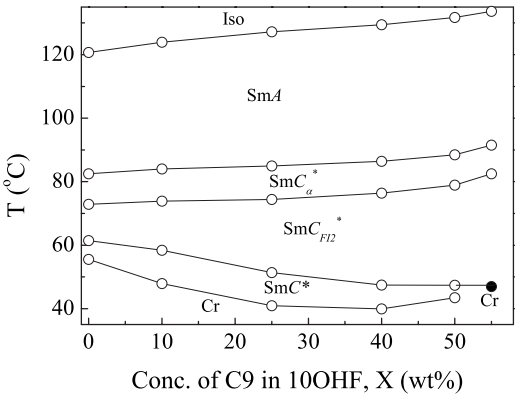

FIG. 9. The phase diagram (temperature vs concentration) of the binary mixtures of the compounds C9 and 10OHF. The points are determined from the temperature dependence of the dielectric permittivity $\epsilon'_{\perp}$ on cooling for a fixed frequency of 1 kHz. Note that the range of SmA and SmC^*_α is not affected by the addition of C9 and for 55 wt. % of C9, the low-temperature SmC^* phase disappears, i.e., no phase sequence reversal is then observed.

that the temperature range of SmA and SmC^*_α are not altered by the change in the concentration of C9. When heated from SmC^* phase the range of SmC^*_{FI2} phase is lower compared to that in the cooling mode. Therefore we conclude that SmC^*_{FI2} phase which is metastable and monotropic in pure 10OHF becomes more stable and exists over a wider temperature range as the concentration of C9 is increased.

IV. PHENOMENOLOGICAL THEORETICAL CONSIDERATION FOR THE PHASE SEQUENCE REVERSAL

The first phenomenological theory for the phase transitions of smectic phases was given by Orihara and Ishibashi [19] in 1990. The various other phenomenological theories have emerged since then for explaining the different experimental results [2,20].

Though details of the phenomenological models vary, a few terms of the free-energy density expression, especially those governing the SmA^*-SmC^* and SmC^*-SmC^*_A transitions are quite similar. For example, a recent model that involves the discrete flexoelectric polarization [21,22], can explain the existence of the various subphases. Free energy can be written as follows:

$$F = \sum_{i=1,2,\ldots}^{N} \left[\tilde{F}_0(\theta) - \tilde{a}\frac{\Delta T}{T^*}(\cos\varphi_{i-1,i} + \cos\varphi_{i,i+1}) - \tilde{B}(\cos^2\varphi_{i-1,i} + \cos^2\varphi_{i,i+1}) + \frac{1}{2\chi}[\mathbf{P}_i^2 + g(\mathbf{P}_i\mathbf{P}_{i+1} + \mathbf{P}_i\mathbf{P}_{i-1})] + c_s(\mathbf{P}_i\boldsymbol{\xi}_i) + c_f\cos\theta(\mathbf{P}_i\Delta\mathbf{n}_{i\pm1}) \right]. \quad (2)$$

Here $\tilde{F}_0(\theta)$ is the tilt angle dependent free energy part that governs the nontilted to a tilted phase transition, that is the SmA^*-SmC^* phase transition. The second and third terms are designed for expressing the synclinic to the anticlinic phase transitions, i.e., SmC^*-SmC^*_A transition. $\Delta T = T - T^*$, where T^* is the transition temperature between the synclinic and anticlinic smectic phases in the absence of other intermediate phases. The last four terms in Eq. (2) involve the polarization $\mathbf{P}$, which is introduced by Osipov *et al.* [21,22] and is devised to explain an emergence of the various subphases. While the last four terms are different and are model dependent and sometimes controversial, the meaning of which are not explained here as these are not concerned with a problem of the phase reversal. The first three terms are rather clear in physical meaning and these appear in slightly different forms in the various phenomenological models based on Landau free energy expansion. The physical meaning of the second and the third terms in this expression can easily be understood, even though the original mechanism is not so simple. The c directors between the neighboring layers are likely to lie in a single plane if the helicity is ignored with positive $\tilde{B}$ (that is, the synclinic or anticlinic orderings), and the ferroelectric and the antiferroelectric configurations are favored by the positive and negative values of the coefficient $\tilde{a}\Delta T/T^*$, respectively. In most compounds and mixtures studied so far, the ferroelectric phase has been observed at a higher temperature than antiferroelectric phase. For this reason $\tilde{a}$ is assumed to be always positive. Note that $\Delta T = T - T^*$ and ΔT is positive for higher temperatures and is negative at lower temperatures than temperature T^*, and as a result, if $\tilde{a}$ is positive, the ferroelectric configuration is stable in a high temperature range. On the contrary, if $\tilde{a}$ is negative, this is stable over a low temperature range. In this way, the phase sequence between the synclinic and anticlinic phases is determined by the coefficient $\tilde{a}$.

Physically, the coefficients $\tilde{a}$ and $\tilde{B}$ originate from the steric and the dipole-dipole interactions between the nearest layers [23]. Both of these interactions contribute to positive $\tilde{B}$, and so, undoubtedly, $\tilde{B}$ is positive. Osipov and Fukuda [22,24] had suggested that the positive $\tilde{a}$ arises from the anisotropic instant dipole-dipole dispersion interactions that favor the anticlinic arrangement whereas the steric favor the synclinic arrangement and contributes to negative $\tilde{a}$. They attributed the instant dipole-dipole interactions or the correlation between the transverse dipoles between the two neighboring layers contributing to the anticlinic arrangement, which depends strongly on temperature and decreasing with increase in temperature. They have also suggested that the steric energy, which favors the synclinic arrangement, is rather independent of temperature and at higher temperatures it dominates the instant dipole-dipole interactions, which in turn is reduced in magnitude by an increase in temperature. According to their model, $\tilde{a}$ should always be positive and the phase sequence reversal cannot appear.

However, an observation of the phase sequence reversal implies that $\tilde{a}$ is actually negative in these particular materials. It is surely not the normal case, but a negative value of $\tilde{a}$ may be possible, though a clear theoretical model where $\tilde{a}$ can be calculated does not exist at this time. We suggest that the steric energy is also strongly temperature dependent, extremely large at low temperatures and it reduces to a low value with increase in temperature. The instant transverse dipole-dipole interaction energy continues to dominate at

higher temperatures. We speculate that the temperature dependence of the steric energy gives rise to negative $\tilde{a}$, i.e., synclinic is favored at low temperatures and anticlinic at high temperatures. This can give rise to the phase reversal sequence observed here.

Although this temperature dependence of the steric energy may appear to be counterintuitive, experimental evidence supports our suggestion. The importance of the steric term was verified experimentally by Lee and Lim [25]. In their paper, the antiferroelectric phase is induced by adding a dopant, the steric energy is reduced by the dopant which acts as a lubricant. This implies that the steric energy depends strongly on the surface morphology of the layers, and so, it is very difficult to describe the strength and its dependence on the temperature accurately with a simple molecular model given by Osipov and Fukuda [24]. Song *et al.* [26] measured the interlayer interaction as a function of temperature in an antiferroelectric material, where the energy barrier (Δ) between the synclinic and anticlinic minima increases and saturates quickly with a reduction in temperature, whereas the spontaneous polarization keeps rising with decreasing temperature for the entire range of temperatures. The measured energy difference Δ shows even a slight decrease at low temperatures. An increasing spontaneous polarization with decreasing temperature implies that the steric energy may keep on increasing with temperature decreasing, and the steric energy could induce the saturation and even decrease Δ with temperature decreasing. This result also shows that the steric energy is temperature dependent and could significantly contribute to the phase reversed behavior as has experimentally been observed here. At higher temperatures the steric energy may indeed be negligible.

Thus, in some materials, $\tilde{a}$ may be negative due to a higher contribution from the steric energy at lower temperatures, and a lower contribution at higher temperatures. In this case the ferroelectric phase exists at a lower temperature, and the antiferroelectric phase exists at higher temperatures. Thus by assuming a negative value for the coefficient $\tilde{a}$, the phase sequence reversal is expected. An addition of the compound in the mixture, that exhibits antiferroelectric phase over a broad range of temperatures leads to the stability in the observed phase-sequence-reversal behavior. For this reason not only does the temperature range of the phase reversed SmC^*_{FI2} phase increase but the addition of this compound also stabilizes this phase and it appears both on cooling and heating.

V. CONCLUSION

Investigations on pure 10OHF sample as well as binary mixtures of 10OHF with 9OTBBB1M7 (C9) confirm the existence of phase sequence reversal SmC^*_α-SmC^*_{FI2}-SmC^* under certain conditions. We find that in the pure 10OHF the high-temperature SmC^*_{FI2} phase is metastable and both the SmC^* and SmC^*_{FI2} are monotropic and these exist only during the cooling mode. The conoscopy figures show that the images of high-temperature SmC^*_{FI2} phase existing in the pure 10OHF compound are unusual and disturbed. The detailed dielectric and polarization studies on binary mixture show that both SmC^* and SmC^*_{FI2} are monotropic in mixtures too but the high-temperature SmC^*_{FI2} phase becomes more stable as the concentration of the C9 is increased. This may suggest that the SmC^*_α-SmC^*_{FI2}-SmC^* phase sequence is not unusual and also 10OHF is not the only compound which exhibits the unusual phase sequence. More compounds that exhibit such a phase reversal need to be discovered and a rigorous theory should evolve to shed more light on this phenomenon.

ACKNOWLEDGMENTS

The authors thank H. T. Srinivasa, Raman Research Institute, Bangalore, India, for assisting in the synthesis of these compounds. K.L.S. thanks IRCSET for support. J.K.S. thanks Samsung Electronics Co., Ltd., for granting a leave of absence from Seoul and SFI is thanked for Grant No. 02/IN.1/I031. We also thank Nissan chemicals, Tokyo for supplying polyimide aligning agent RN1175. We thank Atsuo Fukuda for fruitful discussions.

[1] A. D. L. Chandani, E. Gorecka, Y. Ouchi, H. Takezoe, and A. Fukuda, Jpn. J. Appl. Phys., Part 2 **28**, L1265 (1989).
[2] A. Fukuda, Y. Takanishi, T. Isozaki, K. Ishikawa, and H. Takezoe, J. Mater. Chem. **4**, 997 (1994), and references therein.
[3] E. Gorecka, D. Pociecha, M. Glogarova, and J. Mieczkowski, Phys. Rev. Lett. **81**, 2946 (1998).
[4] P. Mach, R. Pindak, A.-M. Levelut, P. Barois, H. T. Nguyen, C. C. Huang, and L. Furenlid, Phys. Rev. Lett. **81**, 1015 (1998); T. Matsumoto, A. Fukuda, M. Johno, Y. Motoyama, T. Yui, S. S. Seomun, and M. Yamashita, J. Mater. Chem. **9**, 2051 (1999), and references therein.
[5] P. Mach, R. Pindak, A.-M. Levelut, P. Barois, H. T. Nguyen, H. Baltes, M. Hird, K. Toyne, A. J. Seed, J. W. Goodby, C. C. Huang, and L. Furenlid, Phys. Rev. E **60**, 6793 (1999).
[6] Z. Q. Liu, B. K. McCoy, S. T. Wang, R. Pindak, W. Caliebe, P. Barois, P. Fernandes, H. T. Nguyen, and C. S. Hsu, S. Wang, and C. C. Huang, Phys. Rev. Lett. **99**, 077802 (2007).
[7] A. D. L. Chandani, N. M. Shtykov, V. P. Panov, A. V. Emelyanenko, A. Fukuda, and J. K. Vij, Phys. Rev. E **72**, 041705 (2005); N. M. Shtykov, A. D. L. Chandani, A. V. Emelyanenko, A. Fukuda, and J. K. Vij, *ibid.* **71**, 021711 (2005).
[8] S. T. Wang, Z. Q. Liu, B. K. McCoy, R. Pindak, W. Caliebe, H. T. Nguyen, and C. C. Huang, Phys. Rev. Lett. **96**, 097801 (2006).
[9] D. A. Olson, X. F. Han, A. Cady, and C. C. Huang, Phys. Rev. E **66**, 021702 (2002).
[10] M. B. Hamaneh and P. L. Taylor, Phys. Rev. Lett. **93**, 167801 (2004); Phys. Rev. E **72**, 021706 (2005).
[11] K. L. Sandhya, Yu. P. Panarin, U. Manna, J. K. Vij, and S. Kumar, Phys. Rev. Lett. **98**, 219801 (2007).

[12] V. M. Vaksman and Yu. P. Panarin, Mol. Mater. **1**, 147 (1992).
[13] Yu. P. Panarin, O. Kalinovskaya, J. K. Vij, and J. W. Goodby, Phys. Rev. E **55**, 4345 (1997); Yu. P. Panarin, O. Kalinovskaya, and J. K. Vij, Liq. Cryst. **25**, 241 (1998).
[14] In this temperature range the selective reflection spectra for oblique incidence of the light showed two dips: one corresponding to the ordinary selective reflection due to the half pitch (~761–788 nm) and the other due to the full pitch band (1503–1577 nm). These observations are a characteristic feature of SmC^* phase and the temperature above which no dip in the reflection spectra is observed. This rules out the possibility of the high temperature phase being a two-layer one.
[15] J. K. Song, A. D. L. Chandani, O. E. Panarina, A. Fukuda, J. K. Vij, V. Goertz, and J. W. Goodby, Ferroelectrics **344**, 41 (2006).
[16] J. K. Song, J. K. Vij, and I. Kobayashi, Phys. Rev. E **75**, 051705 (2007).
[17] E. Gorecka, A. D. L. Chandani, Y. Ouchi, H. Takezoe, and A. Fukuda, Jpn. J. Appl. Phys., Part 1 **29**, 131 (1990).
[18] K. Miyachi, M. Kabe, K. Ishikawa, H. Takezoe, and A. Fukuda, Ferroelectrics **147**, 147 (1993).
[19] H. Orihara and Y. Ishibashi, Jpn. J. Appl. Phys. **29**, L115 (1990).
[20] M. Yamashita, Mol. Cryst. Liq. Cryst. Sci. Technol., Sect. A **263**, 93 (1995).
[21] A. V. Emelyanenko and M. A. Osipov, Phys. Rev. E **68**, 051703 (2003).
[22] M. A. Osipov, A. Fukuda, and H. Hakoi, Mol. Cryst. Liq. Cryst. **402**, 9 (2003).
[23] M. Čepič and B. Žekš, Phys. Rev. Lett. **87**, 085501 (2001).
[24] M. A. Osipov and A. Fukuda, Phys. Rev. E **62**, 3724 (2000).
[25] J.-H. Lee and T. K. Lim, J. Appl. Phys. **98**, 094110 (2005).
[26] J. K. Song, A. Fukuda, and J. K. Vij, Phys. Rev. E **76**, 011708 (2007).